A SECOND-ORDER CONVEX SPLITTING SCHEME FOR A CAHN-HILLIARD EQUATION WITH VARIABLE INTERFACIAL PARAMETERS*

Xiao Li

Applied and Computational Mathematics Division, Beijing Computational Science Research Center, Beijing 100193, China
Email: lixiao1228@163.com

Zhonghua Qiao

Department of Applied Mathematics, The Hong Kong Polytechnic University, Hung Hom, Kowloon, Hong Kong
Email: zhonghua.qiao@polyu.edu.hk

Hui Zhang

Laboratory of Mathematics and Complex Systems, Ministry of Education and School of Mathematical Sciences, Beijing Normal University, Beijing, China, 100875
Email: hzhang@bnu.edu.cn

Abstract

In this paper, the MMC-TDGL equation, a stochastic Cahn-Hilliard equation with a variable interfacial parameter, is solved numerically by using a convex splitting scheme which is second-order in time for the non-stochastic part in combination with the Crank-Nicolson and the Adams-Bashforth methods. For the non-stochastic case, the unconditional energy stability is obtained in the sense that a modified energy is non-increasing. The scheme in the stochastic version is then obtained by adding the discretized stochastic term. Numerical experiments are carried out to verify the second-order convergence rate for the non-stochastic case, and to show the long-time stochastic evolutions using larger time steps.

Mathematics subject classification: 65M06, 65M12, 65Z05.
Key words: Cahn-Hilliard equation, Second-order accuracy, Convex splitting, Energy stability.

1. Introduction

In this work, we consider a two-dimensional stochastic Cahn-Hilliard equation of the form

$$\frac{\partial \phi}{\partial t} = D\Delta \frac{\delta U(\phi)}{\delta \phi} + \varepsilon \xi(\boldsymbol{r}, t), \quad \boldsymbol{r} \in \Omega, \ t \in (0, T], \tag{1.1}$$

where $\Omega = (0, L_x) \times (0, L_y)$ and $\phi = \phi(\boldsymbol{r}, t)$ is the unknown function subject to the periodic boundary condition. $U(\phi)$ is the Ginzburg-Landau type energy functional of the form

$$U(\phi) = \int_{\Omega} \left(F(\phi) + \kappa(\phi) |\nabla \phi|^2 \right) \mathrm{d}\boldsymbol{r}, \tag{1.2}$$

where $F(\phi)$ is a potential and $\kappa(\phi)$ is the interfacial parameter weighting the gradient energy. The constant $D > 0$ is a diffusion coefficient, and the function $\xi(\boldsymbol{r}, t)$ is a stochastic term representing a kind of noise whose strength is scaled by $\varepsilon > 0$.

In the field of small molecules or polymer mixture systems, the phase transition process has attracted many theoretical and experimental studies [5, 14, 44]. Cahn-Hilliard dynamics, namely (1.1) with $\varepsilon = 0$, proposed by Cahn and Hilliard [4], turns out to be one of the most suitable models for simulating phase transitions of a uniform thermodynamic system [15]. Here, ϕ represents the concentration of one of the components of the mixture (or sometimes, the difference between the concentrations of the two components of a binary mixture [13]). To consider the random disturbance in the system, the stochastic term $\xi(\boldsymbol{r}, t)$ is added into the equation by Cook [7]. In physics, the stochastic term ξ, treated as random force, reflects the thermal disturbance caused by the chaos motion of molecules, and is required to satisfy the fluctuation-dissipation theorem [5, 19]

$$\mathbb{E}[\xi(\boldsymbol{r}_1, t_1)\xi(\boldsymbol{r}_2, t_2)] = -2D\Delta\delta(\boldsymbol{r}_1 - \boldsymbol{r}_2)\delta(t_1 - t_2), \tag{1.3}$$

where $\mathbb{E}$ represents the mathematical expectation operator. The Laplacian in (1.3) expresses the conservation law for the field [17]. A random force component which piles up matter at one site must be exactly balanced by force contributions at neighboring sites which deplete those sites of matter.

In mathematics, the analytical and numerical studies on the stochastic Cahn-Hilliard equation (1.1), also called Cahn-Hilliard-Cook equation, have been investigated by many authors. The existence and regularity of the solutions are proved under some certain conditions [8, 31]. One of the applications of the stochastic Cahn-Hilliard equations is the nucleation and phase transition of the polymer mixtures. In [3], the nucleation is explained by the stochastically driven exit in the limit of small noise intensity from the domain of attraction of an asymptotically stable homogeneous equilibrium state for the associated deterministic model. The process of nucleation by formal arguments using two spatial scales and two temporal scales is described in [2]. In addition, the numerical simulation of the phase transition attracts many attentions. In [17], a class of finite difference schemes are presented and compared with each other for simulating the nucleation in one-, two- and three-dimensional cases. Mesforush et al present the error estimates of the finite element approximations to the Cahn-Hilliard-Cook equation and its linearized version [20, 21]. Spinodal decomposition of binary alloys is studied via Monte-Carlo simulation in [29], considering a two-dimensional system at critical concentration. The so-called string method is adopted to calculate the minimal energy path connecting two metastable states in both one- and two-dimensional cases in [25, 47].

The form of the potential $F(\phi)$ depends on the considered systems. For the phase separation of the small molecules or atomic systems consisting of two components, $F(\phi)$ is usually chosen as a quartic double-well potential function

$$F(\phi) = \frac{1}{4}(\phi^2 - 1)^2, \tag{1.4}$$

where ϕ represents the difference between the concentrations of the two components, and the coefficient $\kappa(\phi)$ is often considered as a positive constant. For the studies of spinodal decomposition in polymer blends, Flory and Huggins developed a lattice theory and gave the Flory-Huggins free energy [11]

$$F(\phi) = \frac{\phi}{N_{\mathrm{A}}} \ln \phi + \frac{1 - \phi}{N_{\mathrm{B}}} \ln(1 - \phi) + \chi\phi(1 - \phi), \tag{1.5}$$

where ϕ is the concentration of the polymer A, N_{A} and N_{B} represent the degree of polymerization of the polymer A and B, respectively, and χ is the Huggins interaction parameter. It is noted in [14] that the gradient energy contribution for the polymer mixtures should be weighted

by

$$\kappa(\phi) = \frac{\sigma^2}{36\phi(1-\phi)}, \tag{1.6}$$

where $\sigma > 0$ is a characteristic monomer length scale. The functional (1.2) with (1.5) and (1.6) is called the Flory-Huggins-de Gennes (FHdG) free energy functional in polymer physics. The phase transition processes of a large class of hydrogels, a kind of network crosslinked by polymer chains, can be described by the equation (1.1) combined with the FHdG energy functional.

A new kind of hydrogels, macromolecular microsphere composite (MMC) hydrogels, are becoming popular in polymeric materials because of their high mechanical strength [18]. The microstructure of MMC hydrogels is composed of both polymer chains and macromolecular microspheres. In [26, 45], a reticular free energy has been developed to describe the structures. Replacing (1.5) in the FHdG energy functional by the reticular free energy and combining the stochastic Cahn-Hilliard equation (1.1), the MMC-TDGL equation is obtained to simulate the phase transition of the MMC hydrogels well. Here, "TDGL" is short for "time-dependent Ginzburg-Landau" and refers to the TDGL mesoscopic simulation methods. We will give the expression of the reticular free energy and the form of the MMC-TDGL equation in Section 2.

The difficulties for the numerical simulation of the Cahn-Hilliard equation are mainly of two aspects: to observe the coarsening dynamics, we need the long-time integration; to capture phase structures at some moments, we need the fine approximations. Therefore, the stability and accuracy of the numerical schemes for the Cahn-Hilliard equation are desirable.

Recently, energy stability has been widely considered for the numerical schemes of the Cahn-Hilliard equation and other phase field models with constant interfacial parameters [9, 12, 16, 22–24, 28, 34, 35, 37, 38, 48]. As one of the energy stable methods, the convex splitting approach, which was firstly proposed by Eyre in his pioneer work [10], has become more and more popular. The basic idea of the convex splitting technique is to decompose the energy into convex and concave parts and then to treat the convex part implicitly while the concave part explicitly. Most convex splitting schemes are of first-order accuracy in time, such as numerical simulations of the Cahn-Hilliard equation [46], the phase field crystal model [43], the epitaxial growth models [6, 41], and the diffuse interface model with Peng-Robinson equation of state [32]. Recently, second-order convex splitting schemes are proposed for the epitaxial growth models [36], where the convex part is approximated by the modified Crank-Nicolson method and the concave part by the second-order Adams-Bashforth formula.

Several works have been done for the models with variable interfacial parameters to investigate some physical properties, such as phase separation and self-assembling. For instance, the growth law for the characteristic domain size during the phase separation is studied by numerical simulations [5]. The aforementioned MMC-TDGL equation is one of the Cahn-Hilliard equation with variable interfacial parameters, and we have investigated some numerical schemes for it in our recent works. A linear semi-implicit difference scheme is derived to simulate the phase transitions of MMC hydrogels in [26]. The stochastic term in (1.1) is discretized in the numerical simulation, and this is the first time for the numerical study for the MMC-TDGL equation. In [27], an unconditionally uniquely solvable and energy stable difference scheme based on the convex splitting method is developed for the non-stochastic case, and the stochastic term is added with the same form as in [26]. Both the linear scheme and the convex splitting scheme are first-order accurate in time, and the numerical results therein suggest that the time steps greater than 10^{-3} are not adequate to the long-time simulations because of the low accuracies.

In this work, motivated partly by [36], we will develop a second-order convex splitting scheme

for a Cahn-Hilliard equation with variable interfacial parameters, namely, the non-stochastic part of the MMC-TDGL equation, which is one aspect of the main contributions of this work. We decompose the energy functional into convex and concave parts by using the same approach in [27], and treat the convex part by the Crank-Nicolson method while the concave part by the second-order Adams-Bashforth formula. The unique solvability comes from the fact that the derived scheme is the Euler-Lagrange equation of a convex functional. However, it is not easy to prove the energy stability via the similar procedure as [36] since the terms involving the variable interfacial parameter are very difficult to address. Instead, as the technique used in [33], we introduce auxiliary variables in the discrete energy functional so that the energy stability will be achieved in the sense that a modified energy is non-increasing. Another aspect of the main contributions is the long-time stochastic simulation with a little larger time step. From the numerical results, we observe the effect of the noise on the long-time coarsening evolutions.

The rest of this paper is organized as follows. In Section 2, we illustrate the mathematical model of the phase transition of the MMC hydrogel. The difference schemes for both non-stochastic and stochastic cases are presented in Section 3. The second-order accuracy is analyzed briefly; the unique solvability and energy stability for the non-stochastic case are proved rigorously. The unique solvability for the stochastic case is the direct consequence. The numerical methods for solving the difference schemes are then discussed. In Section 4, for the non-stochastic case, some numerical experiments are carried out to demonstrate the convergence rate, and the coarsening evolutions are conducted for the stochastic case. Some concluding remarks are given in Section 5.

2. The Mathematical Model: MMC-TDGL Equation

The MMC-TDGL equation is the model (1.1) with the energy functional

$$U(\phi) = \int_\Omega \Big(S(\phi) + H(\phi) + \kappa(\phi)|\nabla\phi|^2 \Big)\, \mathrm{d}\boldsymbol{r}, \tag{2.1}$$

where $S(\phi) + H(\phi)$ is the reticular free energy density [26, 45] with

$$S(\phi) = \frac{\phi}{\gamma}\ln\frac{\alpha\phi}{\gamma} + \frac{\phi}{N}\ln\frac{\beta\phi}{\gamma} + (1-\rho\phi)\ln(1-\rho\phi), \quad H(\phi) = \chi\phi(1-\rho\phi), \tag{2.2}$$

and $\kappa(\phi)$ is the de Gennes coefficient (1.6). Following the notations defined in [26, 45], we denote by χ the Huggins interaction parameter, by N the degree of polymerization of the polymer chains, and by M the relative volume of one macromolecular microsphere which does not appear explicitly in (2.2). The other constants α, β, γ and ρ depend on M and N via

$$\alpha = \pi\Big(\sqrt{\frac{M}{\pi}} + \frac{N}{2}\Big)^2, \quad \beta = \frac{\alpha}{\sqrt{\pi M}}, \quad \gamma = \sqrt{\pi M}N, \quad \rho = 1 + \frac{M}{\gamma}.$$

All these parameters are positive and $0 < \phi < 1/\rho < 1$. We set the diffusion coefficient $D = 1$ in (1.1) for the normalization and the monomer length scale $\sigma = 1$ in (1.6). Let

$$F(\boldsymbol{r}, t) = S(\phi) + H(\phi), \quad K(\boldsymbol{r}, t) = \kappa(\phi)|\nabla\phi|^2, \tag{2.3}$$

then

$$\frac{\partial F}{\partial t} = \big(S'(\phi) + H'(\phi)\big)\phi_t, \quad \frac{\partial K}{\partial t} = \kappa'(\phi)|\nabla\phi|^2\phi_t + 2\kappa(\phi)\nabla\phi\cdot\nabla\phi_t, \tag{2.4}$$

and the energy functional (2.1) can be written as

$$U(t) = \int_\Omega \Big(F(\boldsymbol{r}, t) + K(\boldsymbol{r}, t) \Big)\, \mathrm{d}\boldsymbol{r}.$$

We note that the deterministic Cahn-Hilliard equation, that is, equation (1.1) with $\varepsilon = 0$, has an important property that the energy is non-increasing, i.e.,

$$\frac{\mathrm{d}}{\mathrm{d}t}U(t) \leq 0, \quad t > 0.$$

So we always hope to develop a numerical scheme inheriting such a property.

We have proved in [26] that to meet the condition (1.3), the stochastic term in (1.1) should have the form

$$\xi(\boldsymbol{r}, t) = -\sqrt{2}\,\nabla \cdot \boldsymbol{\eta}(\boldsymbol{r}, t), \tag{2.5}$$

where $\boldsymbol{\eta} = (\eta_1, \eta_2)$ with η_1 and η_2 independent two-dimensional space-time Gaussian white noises, satisfying $\mathbb{E}[\eta_l(\boldsymbol{r}, t)] = 0$ and $\mathbb{E}[\eta_l(\boldsymbol{r}_1, t_1)\eta_l(\boldsymbol{r}_2, t_2)] = \delta(\boldsymbol{r}_1 - \boldsymbol{r}_2)\delta(t_1 - t_2)$, $l = 1, 2$. Noting that the space-time white noise $\boldsymbol{\eta}$ is nowhere differentiable in the common sense, the spatial derivatives of $\boldsymbol{\eta}$ in (2.5) exist in the sense of Schwartz distributions [3, 40].

Now we have given the complete model (1.1) combined with the energy functional (2.1) and the stochastic term (2.5). The numerical simulations show that our model can be used to describe the phase transitions of the microstructures of the MMC hydrogels [26, 27, 45]. A natural question is what the definition or regularity of the solution is. In [31], the regularity of the solution to (1.1) with κ constant is proved under some certain conditions. The authors pointed out that the fourth-order linear part regularizes the solution, the noise makes it worse, and the regularity of the solution depends on the competition of these two terms. In our model, the fourth-order term has stronger regularizing effects because of the contribution of $\kappa(\phi)$ given by (1.6), so we believe the solution has better regularity. Similar to the discussion in [25], we focus on the solutions belonging to $C([0, T]; L^2(\Omega))$.

3. Second-order Convex Splitting Schemes

In this section, we present the convex splitting scheme with second-order accuracy in time for the non-stochastic part of MMC-TDGL equation (1.1) and give the stochastic version by adding the discretized stochastic term into the presented scheme. The unconditional unique solvability and energy stability of the non-stochastic scheme are proved rigorously to ensure the numerical solutions reasonable. And then, the similar results for the stochastic case are also developed. Finally, we give a brief analysis on the numerical methods used to solve the difference schemes.

3.1. Discretization of two-dimensional space

Here we use the similar notations introduced in [42, 43]. Let $h_x = L_x/m$, $h_y = L_y/n$, where $m, n \in \mathbb{N}$. Define the x-direction mesh $x_i = (i - \frac{1}{2})h_x$, $i \in \mathbb{Z}$ in $(0, L_x)$ and the node sets

$$E_m = \{x_{i+\frac{1}{2}} \mid i = 0, 1, \ldots, m\}, \ C_m = \{x_i \mid i = 1, 2, \ldots, m\}, \ C_{\overline{m}} = \{x_i \mid i = 0, 1, \ldots, m+1\}.$$

Similarly, we can define the y-direction mesh $y_j = (j - \frac{1}{2})h_y$, $j \in \mathbb{Z}$ and node sets $E_n, C_n, C_{\overline{n}}$ with respect to $(0, L_y)$. Define the function spaces

$$\mathcal{C}_{m \times n} = \{\phi : C_m \times C_n \to \mathbb{R}\}, \quad \mathcal{C}_{\overline{m} \times \overline{n}} = \{\phi : C_{\overline{m}} \times C_{\overline{n}} \to \mathbb{R}\},$$
$$\mathcal{C}_{\overline{m} \times n} = \{\phi : C_{\overline{m}} \times C_n \to \mathbb{R}\}, \quad \mathcal{C}_{m \times \overline{n}} = \{\phi : C_m \times C_{\overline{n}} \to \mathbb{R}\},$$
$$\mathcal{E}_{m \times n}^{\mathrm{ew}} = \{f : E_m \times C_n \to \mathbb{R}\}, \quad \mathcal{E}_{m \times n}^{\mathrm{ns}} = \{f : C_m \times E_n \to \mathbb{R}\}.$$

The functions in $\mathcal{C}_{m \times n}$, $\mathcal{C}_{\overline{m} \times \overline{n}}$, $\mathcal{C}_{\overline{m} \times n}$ and $\mathcal{C}_{m \times \overline{n}}$ are denoted by the Greek symbols ϕ with $\phi_{i,j} = \phi(x_i, y_j)$. The functions in $\mathcal{E}_{m \times n}^{\mathrm{ew}}$ and $\mathcal{E}_{m \times n}^{\mathrm{ns}}$ are denoted by the English symbols f and g,

respectively. For the function $f \in \mathcal{E}_{m \times n}^{\text{ew}}$, we let $f_{i+\frac{1}{2},j} = f(x_{i+\frac{1}{2}}, y_j)$; for the function $g \in \mathcal{E}_{m \times n}^{\text{ns}}$, we let $g_{i,j+\frac{1}{2}} = g(x_i, y_{j+\frac{1}{2}})$. We say a function $\phi \in \mathcal{C}_{\overline{m} \times \overline{n}}$ is periodic if and only if

$$\phi_{m+1,j} = \phi_{1,j}, \quad \phi_{0,j} = \phi_{m,j}, \quad j = 1, 2, \ldots, n,$$
$$\phi_{i,n+1} = \phi_{i,1}, \quad \phi_{i,0} = \phi_{i,n}, \quad i = 0, 1, \ldots, m+1.$$

Next we define some operators on the function spaces. The averages and differences $a_x, d_x : \mathcal{E}_{m \times n}^{\text{ew}} \to \mathcal{C}_{m \times n}$, $a_y, d_y : \mathcal{E}_{m \times n}^{\text{ns}} \to \mathcal{C}_{m \times n}$, $A_x, D_x : \mathcal{C}_{\overline{m} \times n} \to \mathcal{E}_{m \times n}^{\text{ew}}$, $A_y, D_y : \mathcal{C}_{m \times \overline{n}} \to \mathcal{E}_{m \times n}^{\text{ns}}$, and the two-dimensional discrete Laplacian, $\Delta_h : \mathcal{C}_{\overline{m} \times \overline{n}} \to \mathcal{C}_{m \times n}$, are defined componentwise by

$$a_x f_{i,j} = \frac{1}{2}(f_{i+\frac{1}{2},j} + f_{i-\frac{1}{2},j}), \quad d_x f_{i,j} = \frac{1}{h_x}(f_{i+\frac{1}{2},j} - f_{i-\frac{1}{2},j}), \quad 1 \le i \le m, \ 1 \le j \le n,$$

$$a_y g_{i,j} = \frac{1}{2}(g_{i,j+\frac{1}{2}} + g_{i,j-\frac{1}{2}}), \quad d_y g_{i,j} = \frac{1}{h_y}(g_{i,j+\frac{1}{2}} - g_{i,j-\frac{1}{2}}), \quad 1 \le i \le m, \ 1 \le j \le n,$$

$$A_x \phi_{i+\frac{1}{2},j} = \frac{1}{2}(\phi_{i+1,j} + \phi_{i,j}), \quad D_x \phi_{i+\frac{1}{2},j} = \frac{1}{h_x}(\phi_{i+1,j} - \phi_{i,j}), \quad 0 \le i \le m, \ 1 \le j \le n,$$

$$A_y \phi_{i,j+\frac{1}{2}} = \frac{1}{2}(\phi_{i,j+1} + \phi_{i,j}), \quad D_y \phi_{i,j+\frac{1}{2}} = \frac{1}{h_y}(\phi_{i,j+1} - \phi_{i,j}), \quad 1 \le i \le m, \ 0 \le j \le n,$$

$$\Delta_h \phi_{i,j} = d_x(D_x \phi)_{i,j} + d_y(D_y \phi)_{i,j}, \quad 1 \le i \le m, \ 1 \le j \le n.$$

The weighted inner-product $(\cdot, \cdot)_h$, $[\cdot, \cdot]_{\text{ew}}$ and $[\cdot, \cdot]_{\text{ns}}$ are defined as follows:

$$(\phi, \psi)_h = h_x h_y \sum_{i=1}^{m} \sum_{j=1}^{n} \phi_{i,j} \psi_{i,j}, \quad \phi, \psi \in \mathcal{C}_{m \times n},$$

$$[f, g]_{\text{ew}} = h_x h_y \sum_{i=1}^{m} \sum_{j=1}^{n} a_x(fg)_{i,j}, \quad f, g \in \mathcal{E}_{m \times n}^{\text{ew}},$$

$$[f, g]_{\text{ns}} = h_x h_y \sum_{i=1}^{m} \sum_{j=1}^{n} a_y(fg)_{i,j}, \quad f, g \in \mathcal{E}_{m \times n}^{\text{ns}}.$$

The following proposition follows directly [27, 43].

Proposition 3.1. *Assume that $\phi, \psi \in \mathcal{C}_{\overline{m} \times \overline{n}}$, $f \in \mathcal{E}_{m \times n}^{\text{ew}}$, $g \in \mathcal{E}_{m \times n}^{\text{ns}}$ and ϕ, ψ are periodic, then*
  (1) $[f, A_x \phi]_{\text{ew}} = (a_x f, \phi)_h$, $[f, D_x \phi]_{\text{ew}} = -(d_x f, \phi)_h$;
  (2) $[g, A_y \phi]_{\text{ns}} = (a_y g, \phi)_h$, $[g, D_y \phi]_{\text{ns}} = -(d_y g, \phi)_h$;
  (3) $(\phi, \Delta_h \psi)_h = -[D_x \phi, D_x \psi]_{\text{ew}} - [D_y \phi, D_y \psi]_{\text{ns}} = (\Delta_h \phi, \psi)_h$.

3.2. The difference scheme in the non-stochastic case

The convexity of the integrands in (2.1) is proved in [27], and will be stated below.

Proposition 3.2. (1) *S and $-H$ are convex in $(0, 1/\rho)$, where S and H are defined by (2.2);*
  (2) *$\mathcal{K}(u, v) := \kappa(u)v^2$ is convex in $(0, 1/\rho) \times \mathbb{R}$, where κ is defined by (1.6).*

Now we describe the difference scheme for the MMC-TDGL equation with $\varepsilon = 0$, that is,

$$\frac{\partial \phi}{\partial t} = \Delta \mu, \quad \mu := S'(\phi) + H'(\phi) + \kappa'(\phi)|\nabla \phi|^2 - 2\nabla \cdot \big(\kappa(\phi)\nabla \phi\big). \tag{3.1}$$

To obtain the second-order accuracy, we discrete the equation on the $t_{k+\frac{1}{2}}$-layer. The terms corresponding to $S(\phi)$ and $\kappa(\phi)|\nabla \phi|^2$ are approximated by the Crank-Nicolson method, and the term corresponding to $H(\phi)$ is approximated by the second-order Adams-Bashforth formula.

Introducing a time step $\tau > 0$, for the sequence $\{\psi^k\}_{k\in\mathbb{N}} \subset \mathcal{C}_{\overline{m}\times\overline{n}}$, we define

$$\delta_t\psi^{k+\frac{1}{2}} := \frac{\psi^{k+1} - \psi^k}{\tau}, \quad k = 0, 1, \ldots.$$

The scheme is as follows: given $\phi^k \in \mathcal{C}_{\overline{m}\times\overline{n}}$ periodic, find $\phi^{k+1} \in \mathcal{C}_{\overline{m}\times\overline{n}}$ periodic such that

$$\delta_t\phi^{k+\frac{1}{2}} = \Delta_h\mu^{k+\frac{1}{2}}, \tag{3.2a}$$

$$\begin{aligned}
\mu^{k+\frac{1}{2}} = {}& \widehat{S}^{k+\frac{1}{2}} + \widehat{H}^{k+\frac{1}{2}} + \frac{1}{2}\widehat{\kappa}^{k+1}\big(a_x(D_x\phi^{k+1})^2 + a_y(D_y\phi^{k+1})^2\big) \\
& - d_x(A_x\kappa^{k+1}D_x\phi^{k+1}) - d_y(A_y\kappa^{k+1}D_y\phi^{k+1}) \\
& + \frac{1}{2}\widehat{\kappa}^k\big(a_x(D_x\phi^k)^2 + a_y(D_y\phi^k)^2\big) - d_x(A_x\kappa^kD_x\phi^k) - d_y(A_y\kappa^kD_y\phi^k), \tag{3.2b}
\end{aligned}$$

for $k = 0, 1, \ldots$, where $\kappa^\ell = \kappa(\phi^\ell)$, $\widehat{\kappa}^\ell = \kappa'(\phi^\ell)$, $\ell = k$ or $k+1$, and

$$\widehat{S}^{k+\frac{1}{2}} = \frac{1}{2}\big(S'(\phi^{k+1}) + S'(\phi^k)\big), \qquad k = 0, 1, 2, \ldots, \tag{3.3a}$$

$$\widehat{H}^{k+\frac{1}{2}} = \begin{cases} \dfrac{3}{2}H'(\phi^k) - \dfrac{1}{2}H'(\phi^{k-1}), & k = 1, 2, \ldots, \\[2mm] H'(\phi^0) + \dfrac{\tau}{2}H''(\phi^0)(\phi_t)^0, & k = 0. \end{cases} \tag{3.3b}$$

It is easy to know that the scheme (3.2) is second-order accurate in time as long as the solution to (3.1) is smooth enough. More precisely, we have the following results. The proof is just simple applications of the Taylor formula and we omit it.

Proposition 3.3. *For $k \geq 0$, $\delta_t\phi^{k+\frac{1}{2}}$ is an approximation to $\phi_t(t_{k+\frac{1}{2}})$ with the truncated error*

$$\frac{\tau^2}{24}\big[\phi_{ttt}\big]\big|_{t=t_{k+\frac{1}{2}}} + h.o.t.;$$

$\widehat{S}^{k+\frac{1}{2}}$ defined as (3.3a) is an approximation to $S'(\phi(t_{k+\frac{1}{2}}))$ with the truncated error

$$\frac{\tau^2}{8}\big[S''(\phi)\phi_{tt} + S'''(\phi)(\phi_t)^2\big]\big|_{t=t_{k+\frac{1}{2}}} + h.o.t.;$$

$\frac{1}{2}(\widehat{\kappa}^{k+1}|\nabla\phi^{k+1}|^2 + \widehat{\kappa}^k|\nabla\phi^k|^2)$ is an approximation to $[\kappa'(\phi)|\nabla\phi|^2](t_{k+\frac{1}{2}})$ with the truncated error

$$\frac{\tau^2}{8}\big[(\kappa'(\phi)|\nabla\phi|^2)_t\phi_{tt} + (\kappa'(\phi)|\nabla\phi|^2)_{tt}(\phi_t)^2\big]\big|_{t=t_{k+\frac{1}{2}}} + h.o.t.;$$

$\nabla\cdot(\kappa^{k+1}\nabla\phi^{k+1} + \kappa^k\nabla\phi^k)$ is an approximation to $[2\nabla\cdot(\kappa(\phi)\nabla\phi)](t_{k+\frac{1}{2}})$ with the truncated error

$$\frac{\tau^2}{4}\big[\nabla\cdot(\kappa(\phi)\nabla\phi)_t\phi_{tt} + \nabla\cdot(\kappa(\phi)\nabla\phi)_{tt}(\phi_t)^2\big]\big|_{t=t_{k+\frac{1}{2}}} + h.o.t..$$

For $k \geq 1$, $\widehat{H}^{k+\frac{1}{2}}$ defined as (3.3b) is an approximation to $H'(\phi(t_{k+\frac{1}{2}}))$ with the truncated error

$$-\frac{3\tau^2}{8}\big[H''(\phi)\phi_{tt} + H'''(\phi)(\phi_t)^2\big]\big|_{t=t_{k+\frac{1}{2}}} + h.o.t.;$$

Besides, $\widehat{H}^{\frac{1}{2}}$ is an approximation to $H'(\phi(t_{\frac{1}{2}}))$ with the truncated error

$$\frac{\tau^2}{8}\big[H''(\phi)\phi_{tt} + H'''(\phi)(\phi_t)^2\big]\big|_{t=0} + h.o.t..$$

For the nonlinear difference scheme (3.2), it is necessary to analyze the unique solvability and stability to obtain reasonable numerical solutions.

3.2.1. Unconditional unique solvability

The unique solvability comes from the fact that the scheme (3.2) is the Euler-Lagrange equation of a convex functional.

Lemma 3.1 ([27, 43]) *The operator* $-\Delta_h$ *is positive definite on the space*

$$\mathcal{M}_0 := \{\phi \in \mathcal{C}_{\overline{m} \times \overline{n}} \,|\, \phi \text{ is periodic and } (\phi, 1)_h = 0\}.$$

Lemma 3.2. *Define a functional* $\mathcal{F} : \mathcal{C}_{\overline{m} \times \overline{n}} \to \mathbb{R}$ *as*

$$\mathcal{F}(\phi) = \frac{1}{2}\Big(S(\phi) + \kappa(\phi)\big(a_x(D_x\phi)^2 + a_y(D_y\phi)^2\big), 1\Big)_h,$$

then $\mathcal{F}(\phi)$ *is convex. Furthermore, the variational derivative of* $\mathcal{F}(\phi)$ *is*

$$\frac{\delta \mathcal{F}}{\delta \phi} = \frac{1}{2}S'(\phi) + \frac{1}{2}\kappa'(\phi)\big(a_x(D_x\phi)^2 + a_y(D_y\phi)^2\big) - d_x(A_x\kappa(\phi)D_x\phi) - d_y(A_y\kappa(\phi)D_y\phi).$$

Proof. We know from Proposition 3.2 that $\mathcal{F}(\phi)$ is a linear combination of some convex functions, and thus convex. The variational derivative can be obtained by some simple calculations. □

Theorem 3.1 (Unique solvability) *The difference scheme* (3.2) *is uniquely solvable for any time step* $\tau > 0$.

Proof. The operator $L := -\tau\Delta_h$ is positive definite on $\mathcal{M}_0$, so it is nonsingular and L^{-1} is also positive definite. For given $\phi^k \in \mathcal{M}_0$, define a functional on $\mathcal{M}_0$ as

$$G_k(\phi) = \frac{1}{2}(L^{-1}(\phi), \phi)_h - (L^{-1}(\phi), \phi^k)_h + \mathcal{F}(\phi) + \Big(\frac{1}{2}S'(\phi^k) + \widehat{H}^{k+\frac{1}{2}}, \phi\Big)_h$$
$$+ \Big(\frac{1}{2}\widehat{\kappa}^k\big(a_x(D_x\phi^k)^2 + a_y(D_y\phi^k)^2\big) - d_x(A_x\kappa^k D_x\phi^k) - d_y(A_y\kappa^k D_y\phi^k), \phi\Big)_h.$$

With a little work, we can obtain its variational derivative:

$$\frac{\delta G_k}{\delta \phi} = L^{-1}(\phi - \phi^k) + \frac{1}{2}S'(\phi) + \frac{1}{2}S'(\phi^k) + \widehat{H}^{k+\frac{1}{2}}$$

$$+ \frac{1}{2}\kappa'(\phi)\big(a_x(D_x\phi)^2 + a_y(D_y\phi)^2\big) - d_x(A_x\kappa(\phi)D_x\phi) - d_y(A_y\kappa(\phi)D_y\phi)$$

$$+ \frac{1}{2}\widehat{\kappa}^k\big(a_x(D_x\phi^k)^2 + a_y(D_y\phi^k)^2\big) - d_x(A_x\kappa^k D_x\phi^k) - d_y(A_y\kappa^k D_y\phi^k).$$

For any $\psi \in \mathcal{M}_0$, we have

$$\frac{\mathrm{d}^2 G_k(\phi + \lambda\psi)}{\mathrm{d}\lambda^2}\Big|_{\lambda=0} = (L^{-1}(\psi), \psi)_h + \frac{\mathrm{d}^2 \mathcal{F}(\phi + \lambda\psi)}{\mathrm{d}\lambda^2}\Big|_{\lambda=0}.$$

The convexity of $\mathcal{F}$ and the positive definiteness of L^{-1} imply the strict convexity of G_k on $\mathcal{M}_0$. By noting that the scheme (3.2) is equivalent to the Euler-Lagrange equation of G_k, the unique solvability is the consequence of the strict convexity of G_k. □

3.2.2. Unconditional energy stability

The energy stability will be achieved by considering a modified discrete energy. We define two sequences $\{F^k\}, \{K^k\} \subset \mathcal{C}_{\overline{m} \times \overline{n}}$ generated by

$$F^0 = S(\phi^0) + H(\phi^0), \tag{3.4a}$$

$$\delta_t F^{k+\frac{1}{2}} = (\widehat{S}^{k+\frac{1}{2}} + \widehat{H}^{k+\frac{1}{2}})\delta_t \phi^{k+\frac{1}{2}}, \quad k = 0, 1, \ldots, \tag{3.4b}$$

$$K^0 = \kappa'(\phi^0)\big(a_x(D_x\phi^0)^2 + a_y(D_y\phi^0)^2\big), \tag{3.4c}$$

$$
\begin{aligned}
\delta_t K^{k+\frac{1}{2}} = \frac{1}{2}\Big(&\widehat{\kappa}^{k+1}\big(a_x(D_x\phi^{k+1})^2 + a_y(D_y\phi^{k+1})^2\big) + \widehat{\kappa}^k\big(a_x(D_x\phi^k)^2 \\
&+ a_y(D_y\phi^k)^2\big)\Big)\delta_t\phi^{k+\frac{1}{2}} + \kappa^{k+1}\big(a_x(D_x\phi^{k+1}D_x\delta_t\phi^{k+\frac{1}{2}}) + a_y(D_y\phi^{k+1}D_y\delta_t\phi^{k+\frac{1}{2}})\big) \\
&+ \kappa^k\big(a_x(D_x\phi^k D_x\delta_t\phi^{k+\frac{1}{2}}) + a_y(D_y\phi^k D_y\delta_t\phi^{k+\frac{1}{2}})\big), \quad k = 0, 1, \ldots,
\end{aligned}
\tag{3.4d}
$$

which can be viewed as the discrete form of the equations (2.4).

Theorem 3.2 (Energy stability) *The scheme* (3.2) *is unconditionally energy stable, meaning that for any time step $\tau > 0$, we always have*

$$U_h^{k+1} \le U_h^k,$$

where the discrete energy is defined by $U_h^k = (F^k + K^k, 1)_h$.

Proof. Taking the inner-product of (3.2a) with $\mu^{k+\frac{1}{2}}$ and using Proposition 3.1, we have

$$(\delta_t\phi^{k+\frac{1}{2}}, \mu^{k+\frac{1}{2}})_h = -[D_x\mu^{k+\frac{1}{2}}, D_x\mu^{k+\frac{1}{2}}]_{\text{ew}} - [D_y\mu^{k+\frac{1}{2}}, D_y\mu^{k+\frac{1}{2}}]_{\text{ns}}.$$

Taking the inner-product of (3.2b) with $\delta_t\phi^{k+\frac{1}{2}}$ leads to

$$
\begin{aligned}
(\mu^{k+\frac{1}{2}}, \delta_t\phi^{k+\frac{1}{2}})_h = &(\widehat{S}^{k+\frac{1}{2}} + \widehat{H}^{k+\frac{1}{2}}, \delta_t\phi^{k+\frac{1}{2}})_h \\
&+ \frac{1}{2}\big(\widehat{\kappa}^{k+1}\big(a_x(D_x\phi^{k+1})^2 + a_y(D_y\phi^{k+1})^2\big), \delta_t\phi^{k+\frac{1}{2}}\big)_h \\
&+ \frac{1}{2}\big(\widehat{\kappa}^k\big(a_x(D_x\phi^k)^2 + a_y(D_y\phi^k)^2\big), \delta_t\phi^{k+\frac{1}{2}}\big)_h \\
&- \big(d_x(A_x\kappa^{k+1}D_x\phi^{k+1}) + d_y(A_y\kappa^{k+1}D_y\phi^{k+1}), \delta_t\phi^{k+\frac{1}{2}}\big)_h \\
&- \big(d_x(A_x\kappa^k D_x\phi^k) + d_y(A_y\kappa^k D_y\phi^k), \delta_t\phi^{k+\frac{1}{2}}\big)_h.
\end{aligned}
$$

Using Proposition 3.1, we transform the fourth term in the right-hand-side to

$$
\begin{aligned}
&- \big(d_x(A_x\kappa^{k+1}D_x\phi^{k+1}) + d_y(A_y\kappa^{k+1}D_y\phi^{k+1}), \delta_t\phi^{k+\frac{1}{2}}\big)_h \\
=&[A_x\kappa^{k+1}D_x\phi^{k+1}, D_x\delta_t\phi^{k+\frac{1}{2}}]_{\text{ew}} + [A_y\kappa^{k+1}D_y\phi^{k+1}, D_y\delta_t\phi^{k+\frac{1}{2}}]_{\text{ns}} \\
=&[A_x\kappa^{k+1}, D_x\phi^{k+1}D_x\delta_t\phi^{k+\frac{1}{2}}]_{\text{ew}} + [A_y\kappa^{k+1}, D_y\phi^{k+1}D_y\delta_t\phi^{k+\frac{1}{2}}]_{\text{ns}} \\
=&\big(\kappa^{k+1}, a_x(D_x\phi^{k+1}D_x\delta_t\phi^{k+\frac{1}{2}})\big)_h + \big(\kappa^{k+1}, a_y(D_y\phi^{k+1}D_y\delta_t\phi^{k+\frac{1}{2}})\big)_h \\
=&\big(\kappa^{k+1}, a_x(D_x\phi^{k+1}D_x\delta_t\phi^{k+\frac{1}{2}}) + a_y(D_y\phi^{k+1}D_y\delta_t\phi^{k+\frac{1}{2}})\big)_h.
\end{aligned}
$$

Similarly, the fifth term is transformed to

$$
\begin{aligned}
&- \big(d_x(A_x\kappa^k D_x\phi^k) + d_y(A_y\kappa^k D_y\phi^k), \delta_t\phi^{k+\frac{1}{2}}\big)_h \\
=&\big(\kappa^k, a_x(D_x\phi^k D_x\delta_t\phi^{k+\frac{1}{2}}) + a_y(D_y\phi^k D_y\delta_t\phi^{k+\frac{1}{2}})\big)_h.
\end{aligned}
$$

Then we have

$$
\begin{aligned}
(\mu^{k+\frac{1}{2}}, \delta_t\phi^{k+\frac{1}{2}})_h &= (\widehat{S}^{k+\frac{1}{2}} + \widehat{H}^{k+\frac{1}{2}}, \delta_t\phi^{k+\frac{1}{2}})_h \\
&\quad + \frac{1}{2}\big(\widehat{\kappa}^{k+1}\big(a_x(D_x\phi^{k+1})^2 + a_y(D_y\phi^{k+1})^2\big), \delta_t\phi^{k+\frac{1}{2}}\big)_h \\
&\quad + \frac{1}{2}\big(\widehat{\kappa}^{k}\big(a_x(D_x\phi^{k})^2 + a_y(D_y\phi^{k})^2\big), \delta_t\phi^{k+\frac{1}{2}}\big)_h \\
&\quad + \big(\kappa^{k+1}, a_x(D_x\phi^{k+1}D_x\delta_t\phi^{k+\frac{1}{2}}) + a_y(D_y\phi^{k+1}D_y\delta_t\phi^{k+\frac{1}{2}})\big)_h \\
&\quad + \big(\kappa^{k}, a_x(D_x\phi^{k}D_x\delta_t\phi^{k+\frac{1}{2}}) + a_y(D_y\phi^{k}D_y\delta_t\phi^{k+\frac{1}{2}})\big)_h \\
&= (\delta_t F^{k+\frac{1}{2}}, 1)_h + (\delta_t K^{k+\frac{1}{2}}, 1)_h = \delta_t U_h^{k+\frac{1}{2}}.
\end{aligned}
$$

As a result, we obtain

$$
\delta_t U_h^{k+\frac{1}{2}} = -[D_x\mu^{k+\frac{1}{2}}, D_x\mu^{k+\frac{1}{2}}]_{\text{ew}} - [D_y\mu^{k+\frac{1}{2}}, D_y\mu^{k+\frac{1}{2}}]_{\text{ns}} \le 0,
$$

which completes the proof. $\square$

3.3. The difference scheme in the stochastic case

Now we describe the difference scheme for the case $\varepsilon > 0$. We first recall the discretization of the stochastic term (2.5). See [26] in detail (see also [1]).

As is known to us, the space-time Gaussian white noise can be expressed as dW/dt, where $W(t)$ is the Brownian motion on $L^2(\Omega)$. Separating the variables of W, we obtain

$$
W(t, x, y) = \sum_{p,q\in\mathbb{Z}} \beta_{pq}(t)e_{pq}(x, y), \quad (x, y) \in \Omega,\ t \ge 0,
$$

where $\{e_{pq}\}$ is a set of normal orthogonal basis on $L^2(\Omega)$, $\beta_{pq}(t) = (W(t), e_{pq})_{L^2(\Omega)}$, and $\{\beta_{pq}(t)\}$ is a sequence of independent Wiener process, thus

$$
\frac{\beta_{pq}(t_{k+1}) - \beta_{pq}(t_k)}{\sqrt{\tau}} \sim N(0, 1).
$$

Using the mid-rectangle quadrature formula, we approximate $\eta_{ij}^{k+\frac{1}{2}}$ (either $(\eta_1)_{ij}^{k+\frac{1}{2}}$ or $(\eta_2)_{ij}^{k+\frac{1}{2}}$) as

$$
\begin{aligned}
\eta_{ij}^{k+\frac{1}{2}} = \Big(\frac{dW}{dt}\Big)_{ij}^{k+\frac{1}{2}} &\approx \frac{1}{h_xh_y\tau} \int_{(i-\frac{1}{2})h_x}^{(i+\frac{1}{2})h_x} \int_{(j-\frac{1}{2})h_y}^{(j+\frac{1}{2})h_y} \int_{t_k}^{t_{k+1}} \frac{dW}{dt}\, dxdydt \\
&= \frac{1}{h_xh_y\tau} \sum_{p,q\in\mathbb{Z}} (\beta_{pq}(t_{k+1}) - \beta_{pq}(t_k)) \int_{(i-\frac{1}{2})h_x}^{(i+\frac{1}{2})h_x} \int_{(j-\frac{1}{2})h_y}^{(j+\frac{1}{2})h_y} e_{pq}\, dxdy.
\end{aligned}
$$

For $i = 1, \ldots, m$ and $j = 1, \ldots, n$, we choose

$$
e_{ij} = \frac{1}{\sqrt{h_xh_y}}\mathbf{1}_{[(i-\frac{1}{2})h_x, (i+\frac{1}{2})h_x)\times[(j-\frac{1}{2})h_y, (j+\frac{1}{2})h_y)}.
$$

For $p \ne i$ or $q \ne j$, by orthogonalizing the basis functions, we obtain

$$
\int_{(i-\frac{1}{2})h_x}^{(i+\frac{1}{2})h_x} \int_{(j-\frac{1}{2})h_y}^{(j+\frac{1}{2})h_y} e_{pq}\, dxdy = 0.
$$

Then we have

$$
\eta_{ij}^{k+\frac{1}{2}} \approx \frac{1}{h_xh_y\tau}(\beta_{ij}(t_{k+1}) - \beta_{ij}(t_k))\sqrt{h_xh_y}
$$

$$= \frac{1}{\sqrt{h_x h_y \tau}} \frac{\beta_{ij}(t_{k+1}) - \beta_{ij}(t_k)}{\sqrt{\tau}} = \frac{1}{\sqrt{h_x h_y \tau}} r_{ij}^{k+\frac{1}{2}},$$

where $\{r_{ij}^{k+\frac{1}{2}}\}$ is a sequence of standard normal random variables. Therefore, the discretized form of the stochastic term (2.5) is

$$\xi_{ij}^{k+\frac{1}{2}} = -\frac{\sqrt{2}}{\sqrt{h_x h_y \tau}} \Big(a_x D_x (r_1)_{ij}^{k+\frac{1}{2}} + a_y D_y (r_2)_{ij}^{k+\frac{1}{2}} \Big), \tag{3.5}$$

where $(r_l)^{k+\frac{1}{2}} = \{(r_l)_{ij}^{k+\frac{1}{2}} : 1 \le i \le m, \ 1 \le j \le n\}$ $(l = 1, 2)$ is a sequence of standard normal random variables.

The difference scheme is presented as follows: given $\phi^k \in \mathcal{C}_{\overline{m} \times \overline{n}}$ periodic, find $\phi^{k+1} \in \mathcal{C}_{\overline{m} \times \overline{n}}$ periodic such that

$$\delta_t \phi^{k+\frac{1}{2}} = \Delta_h \mu^{k+\frac{1}{2}} + \varepsilon \xi^{k+\frac{1}{2}}, \tag{3.6}$$

where $\mu^{k+\frac{1}{2}}$ is still expressed as (3.2b), and $\xi^{k+\frac{1}{2}} = \{\xi_{ij}^{k+\frac{1}{2}} : 1 \le i \le m, \ 1 \le j \le n\}$ with components given by (3.5). Note that the stochastic term $\xi^{k+\frac{1}{2}}$ does not depend on the unknown ϕ^{k+1}, so the unique solvability of (3.6) is the direct corollary of Theorem 3.1.

Corollary 3.1 (Unique solvability) *The difference scheme* (3.6) *is uniquely solvable for any time step* $\tau > 0$.

Remark 3.1. We cannot claim that the stochastic scheme (3.6) is second-order convergent in the strong or weak sense. The common way to estimate the truncated error is to use the Taylor formula in the stochastic sense, which is different from the deterministic Taylor formula, so it is illegal to obtain the convergence results directly from the deterministic case. The construction of the second-order difference scheme for the stochastic case may be another big job, therefore, we just use (3.6) for simulation in this paper without considering the convergence.

3.4. Newton-BiCGSTAB method

Here we discuss the numerical methods for solving the difference schemes (3.2) and (3.6). The proof of Theorem 3.1 or Corollary 3.1 indicates that ϕ^{k+1} is the unique minimum of a convex functional G_k, so we can use the optimization method to minimize the objective functional. We adopt the standard Newton method (see, e.g., [30]) to search the minimum and the BiCGSTAB method [39] to solve the Newton equation.

For convenience of the statement, we view the functional G_k as an mn-variable function. The procedure for finding ϕ^{k+1} with given ϕ^k is as follows:

1. Let $\phi^{(0)} = \phi^k$ and $\phi^{(l)}$ is the l-th iterations of ϕ^{k+1};

2. Solving the system $\nabla^2 G_k(\phi^{(l)}) \psi^{(l)} = -\nabla G_k(\phi^{(l)})$ by BiCGSTAB method;

3. Let $\phi^{(l+1)} = \phi^{(l)} + \psi^{(l)}$;

4. If $\|\psi^{(l)}\| < \text{tol}$, let $\phi^{k+1} = \phi^{(l+1)}$; otherwise, let $l = l + 1$ and turn to step 2.

The Newton equation $\nabla^2 G_k(\phi) \psi = -\nabla G_k(\phi)$ can be rewritten as

$$\psi - \tau \Delta_h \big(\mathcal{A}(\phi)\psi\big)$$
$$= -(\phi - \phi^k - \tau \varepsilon \xi^{k+\frac{1}{2}}) + \tau \Delta_h \Big(\frac{1}{2} S'(\phi) + \frac{1}{2} S'(\phi^k) + \widehat{H}^{k+\frac{1}{2}}$$

$$+ \frac{1}{2}\kappa'(\phi)\big(a_x(D_x\phi)^2 + a_y(D_y\phi)^2\big) - d_x(A_x\kappa(\phi)D_x\phi) - d_y(A_y\kappa(\phi)D_y\phi)$$

$$+ \frac{1}{2}\widehat{\kappa}^k\big(a_x(D_x\phi^k)^2 + a_y(D_y\phi^k)^2\big) - d_x(A_x\kappa^k D_x\phi^k) - d_y(A_y\kappa^k D_y\phi^k)\Big),$$

where $\mathcal{A}(\phi) := \frac{1}{h_x h_y}\nabla^2\mathcal{F}(\phi)$ and

$$\mathcal{A}(\phi)\psi = \frac{1}{2}\Big(S''(\phi) + \kappa''(\phi)\big(a_x(D_x\phi)^2 + a_y(D_y\phi)^2\big)\Big)\psi + \kappa'(\phi)\big(a_x(D_x\phi D_x\psi) + a_y(D_y\phi D_y\psi)\big)$$

$$- d_x\big(A_x(\kappa'(\phi)\psi)D_x\phi + A_x\kappa(\phi)D_x\psi\big) - d_y\big(A_y(\kappa'(\phi)\psi)D_y\phi + A_y\kappa(\phi)D_y\psi\big).$$

The system of equations with respect to the Newton step ψ is large and sparse, and thus, can be solved by the BiCGSTAB method.

4. Numerical Experiments

Our experiments are divided into two parts. First, we conduct convergence tests in the non-stochastic case $\varepsilon = 0$ for both the second-order difference scheme (3.2) and the first-order scheme developed in [27]. Second, we use the difference scheme (3.6) to simulate the MMC-TDGL equation (1.1) with various noise strengths $\varepsilon > 0$. It is aim to observe the effects of the noise on the long-time coarsening evolutions.

All the following experiments are carried out on the domain $\Omega = (0, 50) \times (0, 50)$ with the 200×200 mesh nodes. We set $M = 0.16$ and $N = 4.34$ in the model. The tolerance of the Newton iteration is set to be 10^{-6} and the tolerance of the BiCGSTAB method for solving the Newton equation is 10^{-8}.

4.1. Convergence tests

We first present convergence tests on the second-order scheme (3.2) and compare with the first-order scheme presented in our recent work [27]. For the comparison, we use the second-order scheme with a very small time step to give an "exact" solution for both cases. The initial condition is set to be

$$\phi(x, y, 0) = 0.6 + 0.1\bigg(\sin\frac{6\pi x}{L_x}\sin\frac{4\pi y}{L_y} + \sin\frac{10\pi x}{L_x}\sin\frac{10\pi y}{L_y}\bigg)$$

with $L_x = L_y = 50$, and the Huggins parameter is set to be $\chi = 2.37$.

We conduct the experiments with the time steps $\tau = 64\delta, 32\delta, 16\delta, 8\delta, 4\delta, 2\delta, \delta$ with $\delta = 2.5 \times 10^{-4}$. The length of the time interval T is set to be $T = 6400\delta = 1.6$. The "exact" solution is calculated by the second-order scheme (3.2) with a smaller time step $\tau = \delta/5 = 5 \times 10^{-5}$.

Numerical results on the L^∞, L^2 and energy errors are shown in Table 4.1. In the table, the L^∞ error refers to the maximum of the absolute difference between the numerical and "exact" solutions, the L^2 error refers to the discrete L^2 norm of the difference between the numerical and "exact" solutions, and the energy error refers to the absolute difference between the energies of the numerical and "exact" solutions. The convergence rate is the base 2 logarithm of the ratio of the error for the current time step and the error for the preceding larger time step.

It is easy to see that both the two schemes reach gradually the optimal convergence rates as the time steps decrease. Comparing the error values, we see that the second-order scheme is far more accurate than the first-order scheme. To obtain a given accuracy, we can use ten to hundred times larger time steps in the second-order scheme (3.2) than in the first-order scheme [27].

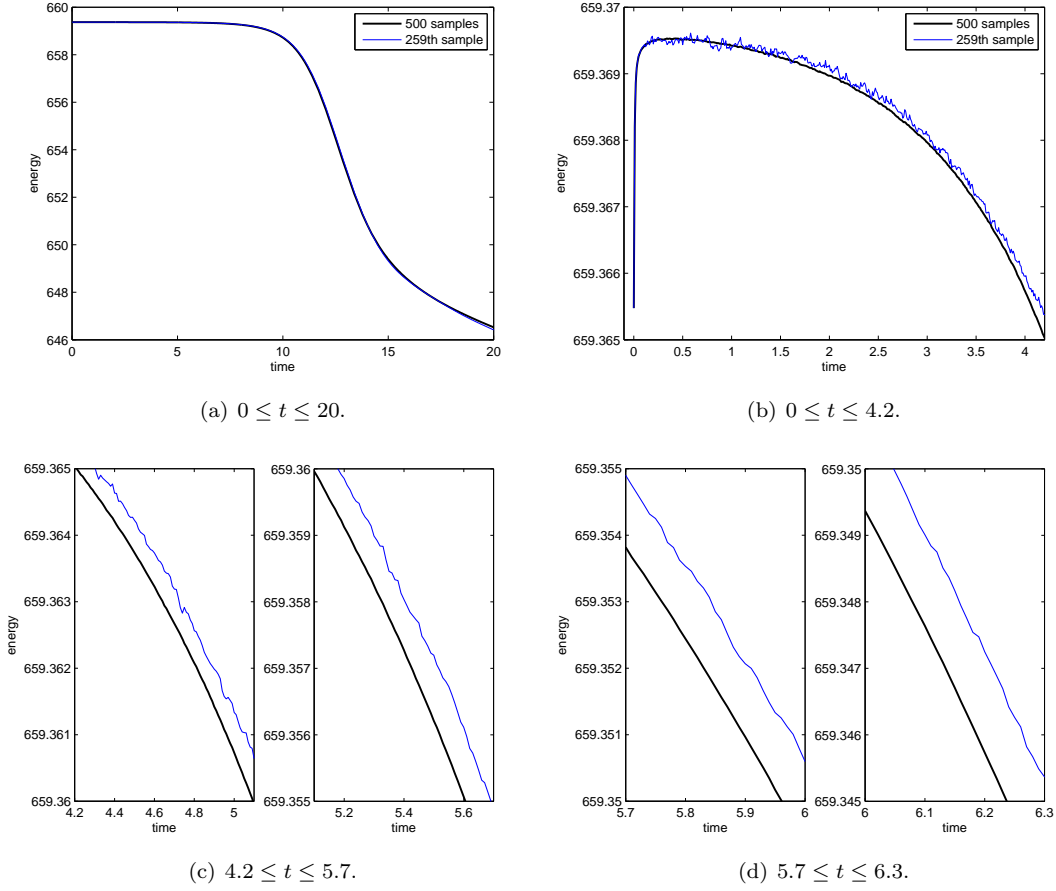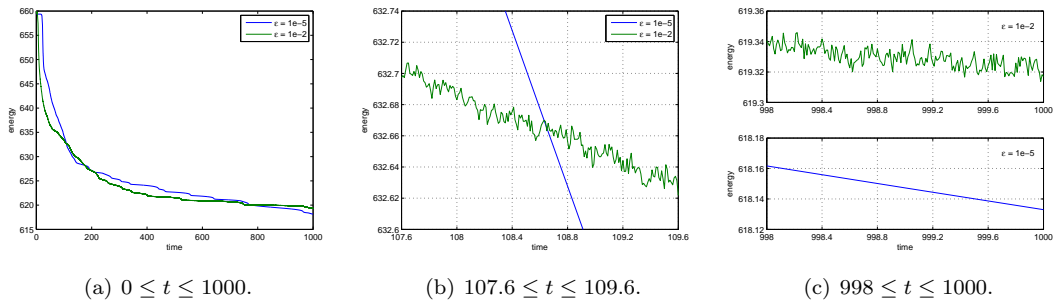## 4.2. Stochastic simulations

To observe the evolutions driven by the stochastic term, we simulate the MMC-TDGL equation using the scheme (3.6) with the time step $\tau = 0.01$ for the long-time coarsening evolutions. Here, we set the initial state to be uniform and metastable, i.e., $\phi(x, y, 0) \equiv 0.3$, and choose $\chi = 1.975$ in the model.

First, we are interested in the energy evolutions in the mean sense though we do not obtain theoretical results about it. Here, we adopt the classical Monte Carlo method to compute the expectations. Driven by the noise with strength $\varepsilon = 10^{-3}$, the system escapes away from the initial state and the phase transition is observed. We focus on the time interval $[0, 20]$ where the first obvious phase transition occurs. Fig. 4.1 plots the mean energy (bold black curve) of 500 independent samples and the energy of one sample (thin blue curve) which has the largest L^2-deviation from the mean value. The black curve is almost smooth throughout the considered interval, and the blue curve performs as the whole trend similar to the black one with the obvious oscillations at some moments. For the comparison, the scales of y-axis in Fig. 4.1(b), (c) and (d) are set to be identical. In the mean sense, the system driven by the noise climbs over an energy barrier from the beginning to about $t = 0.5$, which is manifested as the increasing of the energy, see Fig. 4.1(b). After the system escapes away from the initial metastable state, the energy turns to decrease more and more sharply, that is, the phase transition occurs generally. We observe from Fig. 4.1(c) and (d) that the oscillations on the blue curve are weaker and weaker as the time evolves and vanish after about $t = 5.7$, which is because the phase transits so rapidly that the noise has little effect on the process. The whole process is the performance of the noise driving, which is consistent with the results given in [47].

Second, we are concerned about the phase transition processes driven by the noises with different strengths. We consider the noise with $\varepsilon = 10^{-5}$ as the "small" noise while the noise with $\varepsilon = 10^{-2}$ as the "big" one. The energy evolutions up to the time $T = 1000$ are presented in Fig. 4.2. We observe from Fig. 4.2(a) that the system driven by the big noise climbs over a larger energy barrier and starts the phase transition earlier than the small noise case, which is consistent with the phenomena we have observed in the previous works (see [26,27]). Moreover, some local details of the energy evolution curves are shown in Fig. 4.2(b) and (c), where the

Table 4.1: Numerical errors and convergence rates.

τ	1.6×10^{-2}	8×10^{-3}	4×10^{-3}	2×10^{-3}	1×10^{-3}	5×10^{-4}	2.5×10^{-4}
1st-order							
L^∞ error	9.8852e-2	5.4327e-2	2.8080e-2	1.4191e-2	7.1210e-3	3.5651e-3	1.7835e-3
rate	*	0.8636	0.9521	0.9845	0.9948	0.9981	0.9992
L^2 error	9.9907e-1	5.1794e-1	2.6344e-1	1.3281e-1	6.6673e-2	3.3403e-2	1.6718e-2
rate	*	0.9478	0.9753	0.9881	0.9942	0.9971	0.9986
energy error	4.2765	2.1497	1.0773	5.3915e-1	2.6967e-1	1.3486e-1	6.7433e-2
rate	*	0.9923	0.9967	0.9987	0.9995	0.9998	0.9999
2nd-order							
L^∞ error	1.4756e-3	3.7236e-4	9.3448e-5	2.3396e-5	5.8444e-6	1.4516e-6	3.5317e-7
rate	*	1.9865	1.9945	1.9979	2.0011	2.0094	2.0392
L^2 error	1.4834e-2	3.7064e-3	9.2691e-4	2.3172e-4	5.7837e-5	1.4354e-5	3.4824e-6
rate	*	2.0008	1.9995	2.0001	2.0023	2.0105	2.0433
energy error	5.1736e-2	1.2972e-2	3.2482e-3	8.1244e-4	2.0283e-4	5.0344e-5	1.2213e-5
rate	*	1.9958	1.9977	1.9993	2.0020	2.0104	2.0434

(a) $0 \leq t \leq 20$.

(b) $0 \leq t \leq 4.2$.

(c) $4.2 \leq t \leq 5.7$.

(d) $5.7 \leq t \leq 6.3$.

Fig. 4.1. Energy evolutions of 500 samples with $\varepsilon = 10^{-3}$.

(a) $0 \leq t \leq 1000$.

(b) $107.6 \leq t \leq 109.6$.

(c) $998 \leq t \leq 1000$.

Fig. 4.2. Energy evolutions with $\varepsilon = 10^{-5}$ and 10^{-2}.

same scale is adopted in the coordinate axes for the comparison. It is obvious that the curve corresponding to the big noise performs oscillations almost everywhere while the curve corresponding to the small noise preforms smoothly, no matter whether the energy decreases fast (Fig. 4.2(b)) or slowly (Fig. 4.2(c)). This is because the geometric evolution dominates during the phase transition process driven by the small noise, while the noise dominates in the big noise case. We can also observe such effect of the noise from the solutions at some moments.
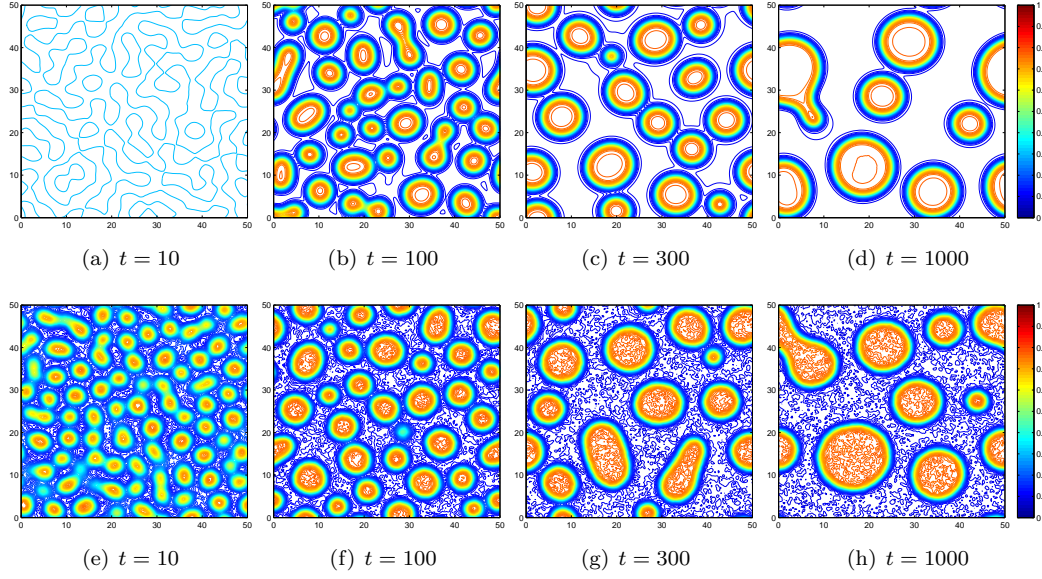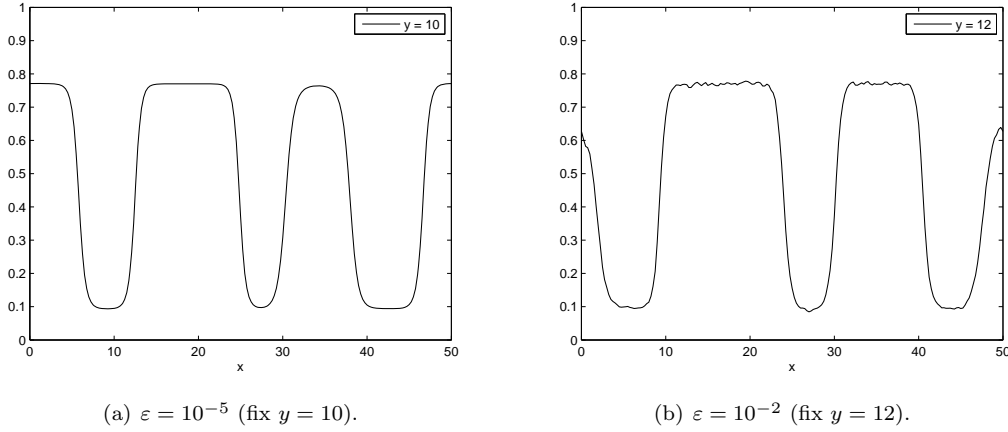
(a) $t = 10$ (b) $t = 100$ (c) $t = 300$ (d) $t = 1000$

(e) $t = 10$ (f) $t = 100$ (g) $t = 300$ (h) $t = 1000$

Fig. 4.3. Evolutions with $\varepsilon = 10^{-5}$ (up) and 10^{-2} (below).

(a) $\varepsilon = 10^{-5}$ (fix $y = 10$).   (b) $\varepsilon = 10^{-2}$ (fix $y = 12$).

Fig. 4.4. Solutions at $t = 1000$ with $\varepsilon = 10^{-5}$ and 10^{-2}.

Fig. 4.3 shows the contour graphs of the solutions at $t = 10, 100, 300$ and 1000. In the domain which one phase occupies, the solutions perform flat and smooth for the small noise case (see Fig. 4.3(a)-(d)) while many oscillations are observed for the big noise case (see Fig. 4.3(e)-(h)), which can be also seen from the cross section curves of the final solutions by fixing y (see Fig. 4.4). That is still the performance of the noise driving, similar to the phenomena observed in [47].

We also observe the evolutions of the phase structures from Fig. 4.3, where the red parts in the graphs represent the chain-rich domains. Here, the initial concentration of the segments has been set as 0.3. Because of the lack of the segments, the polymer chains grafted on the surface of the microspheres are too short to entangle with the chains on the other microspheres. Every microspheres with chains on its surface dissociate each other in the solvent, so we observe that the red parts constitute some isolated balls. In this paper, we mainly focus on the effects

of different noises on the longtime evolutions using the second-order schemes, and thus, only the case $\phi(\boldsymbol{r}, 0) = 0.3$ was simulated. In our previous work [26], we simulated more cases with different concentrations of the segments, and in the case $\phi(\boldsymbol{r}, 0) = 0.6$ we observed the crosslink networks, consistent with the microstructure of the MMC hydrogels [18].

5. Conclusions

In this paper, we develop a second-order convex splitting scheme for a Cahn-Hilliard equation with variable interfacial parameters in combination with the Crank-Nicolson and Adams-Bashforth discretization. The unique solvability is proved by constructing a convex functional whose Euler-Lagrange equation is equivalent to the proposed scheme. By introducing auxiliary variables F and K, we define the energy in an alternate way to avoid the difficulty for the energy stability in the classical theories. Since the auxiliary variables F and K are updated by (3.4), which is based on the evolutionary equations (2.4) instead of the original expressions (2.3), the energy stability is obtained with respect to a modified energy U_h. The second-order accuracy of the derived scheme is demonstrated numerically in the non-stochastic case and compared with the convergence rate of the scheme presented in [27]. The main advantage of the proposed scheme is the second-order accuracy in time so that larger time steps can be used in the long-time simulations.

We did not consider the second-order scheme for the stochastic case, instead, we added directly the stochastic term into the scheme for the deterministic case. In fact, one could use the Taylor formula in the stochastic case, derived from the Itô formula, to construct second-order schemes, which is out of range of this paper, so we leave it as one of our future works.

We should point out that we do not use the technique of convex splitting to prove the energy stability directly. The energy stability we obtain in this work is just based on the modified energy U_h instead of the original energy (2.1), so in fact, we obtain $U(\phi^{k+1}) \leq U(\phi^k) + \mathcal{O}(\tau^2)$, which is similar to the energy identity obtained in [36]. One of the future works in this direction is to develop second-order accurate energy stable schemes based on a direct discretization of the energy (2.1). Other future works include the high-order linear energy stable schemes, which is important in improving the efficiency of the simulations for the complicated nonlinear equations. In addition, we do not work out the energy stability in the stochastic case because it will involve the Itô integrals, which is left as another future work.

References

[1] E.J. Allen, S.J. Novosel and Z. Zhang, Finite element and difference approximation of some linear stochastic partial differential equations, *Stochastics and Stochastic Reports*, **64** (1998), 117-142.

[2] P.W. Bates and P.C. Fife, The dynamics of nucleation for the Cahn-Hilliard equation, *SIAM J. Appl. Math.*, **53** (1993), 990-1008.

[3]   D. Blömker, B. Gawron and T. Wanner, Nucleation in the one-dimensional stochastic Cahn-Hilliard model, *Discrete Cont. Dyn. Sys. A*, **27** (2010), 25-52.

[4]   J.W. Cahn and J.E. Hilliard, Free energy of a nonuniform system. I. Interfacial free energy, *J. Chem. Phys.*, **28** (1958), 258-267.

[5]   A. Chakrabarti, R. Toral, J.D. Gunton and M. Muthukumar, Dynamics of phase separation in a binary polymer blend of critical composition, *J. Chem. Phys.*, **92** (1990), 6899-6909.

[6]   W.B. Chen, S. Conde, C. Wang, X.M. Wang and S.M. Wise, A linear energy stable scheme for a thin film model without slope selection, *J. Sci. Comput.*, **52** (2012), 546-562.

[7]   H. Cook, Brownian motion in spinodal decomposition, *Acta Metall.*, **18** (1970), 297-306.

[8]   A. Debussche and L. Zambotti, Conservative stochastic Cahn-Hilliard equation with reflection, *Ann. Probab.*, **35** (2007), 1706-1739.

[9]   Q. Du and R.A. Nicolaides, Numerical analysis of a continuum model of phase transition, *SIAM J. Numer. Anal.*, **28** (1991), 1310-1322.

[10] D.J. Eyre, Unconditionally gradient stable time marching the Cahn-Hilliard equation, in *Computational and Mathematical Models of Microstructural Evolution*, J. W. Bullard, R. Kalia, M. Stoneham, and L. Q. Chen (eds.), Mater. Res. Soc. Symp. Proc. 529, Materials Research Society, Warrendale, PA, 1998, 39-46.

[11] P.J. Flory, Principles of Polymer Chemistry, Cornell University Press, New York, 1953.

[12] D. Furihata, A stable and conservative finite difference scheme for the Cahn-Hilliard equation, *Numer. Math.*, **87** (2001), 675-699.

[13] H. Garcke, Mechanical effects in the Cahn-Hilliard model: A review on mathematical results, in *Mathematical methods and models in phase transitions*, A. Miranville (ed.), Nova Sci. Publ., New York, 2005, 43-77.

[14] P.G. de Gennes, Dynamics of fluctuations and spinodal decomposition in polymer blends, *J. Chem. Phys.*, **72** (1980), 4756-4763.

[15] S.C. Glotzer and W. Paul, Molecular and mesoscale simulation methods for polymer materials, *Annu. Rev. Mater. Res.*, **32** (2002), 401-436.

[16] R.H. Guo, L.Y. Ji and Y. Xu, High order local discontinuous Galerkin methods for the Allen-Cahn equation: Analysis and simulation, *J. Comput. Math.*, **34** (2016), 135-158.

[17] K.A. Hawick and D.P. Playne, Modelling and visualizing the Cahn-Hilliard-Cook equation, *Tech. rep.*, Computer Science, Massey University, 2008, CSTN-049.

[18] T. Huang, H.G. Xu, K.X. Jiao, L.P. Zhu, H.R. Brown and H.L. Wang, A novel hydrogel with high mechanical strength: A macromolecular microsphere composite hydrogel, *Adv. Mater.*, **19** (2007), 1622-1626.

[19] M. Ibañes, J. García-Ojalvo, R. Toral and J.M. Sancho, Noise-induced phase separation: Mean-field results, *Phys. Rev. E*, **60** (1999), 3597-3605.

[20] M. Kovács, S. Larsson and A. Mesforush, Finite element approximation of the Cahn-Hilliard-Cook equation, *SIAM J. Numer. Anal.*, **49** (2011), 2407-2429.

[21] S. Larsson and A. Mesforush, Finite-element approximation of the linearized Cahn-Hilliard-Cook equation, *IMA J. Numer. Anal.*, **31** (2011), 1315-1333.

[22] D. Li and Z.H. Qiao, On second order semi-implicit Fourier spectral methods for 2D Cahn-Hilliard equations, *J. Sci. Comput.*, **70** (2017), 301-341.

[23] D. Li and Z.H. Qiao, On the stabilization size of semi-implicit Fourier-spectral methods for 3D Cahn-Hilliard equations, *Commun. Math. Sci.*, **15** (2017), 1489-1506.

[24] D. Li, Z.H. Qiao and T. Tang, Characterizing the stabilization size for semi-implicit Fourier-spectral method to phase field equations, *SIAM J. Numer. Anal.*, **54** (2016), 1653-1681.

[25] T.J. Li, P.W. Zhang and W. Zhang, Nucleation rate calculation for the phase transition of diblock copolymers under stochastic Cahn-Hilliard dynamics, *Multiscale Model. Simul.*, **11** (2013), 385-409.

[26] X. Li, G.H. Ji and H. Zhang, Phase transitions of macromolecular microsphere composite hydrogels

based on the stochastic Cahn-Hilliard equation, *J. Comput. Phys.*, **283** (2015), 81-97.

[27] X. Li, Z.H. Qiao and H. Zhang, An unconditionally energy stable finite difference scheme for a stochastic Cahn-Hilliard equation, *Sci. China Math.*, **59** (2016), 1815-1834.

[28] F.S. Luo, T. Tang and H.H. Xie, Parameter-free time adaptivity based on energy evolution for the Cahn-Hilliard equation, *Commun. Comput. Phys.*, **19** (2016), 1542-1563.

[29] A. Milchev, D.W. Heermann and K. Binder, Monte-Carlo simulation of the Cahn-Hilliard model of spinodal decomposition, *Acta Metall.*, **36** (1988), 377-383.

[30] J. Nocedal and S.J. Wright, Numerical Optimization, Springer-Verlag, New York, 1999.

[31] G. Da Prato and A. Debussche, Stochastic Cahn-Hilliard equation, *Nonlinear Anal.*, **26** (1996), 241-263.

[32] Z.H. Qiao and S.Y. Sun, Two-phase fluid simulation using a diffuse interface model with Peng-Robinson equation of state, *SIAM J. Sci. Comput.*, **36** (2014), B708-B728.

[33] Z.H. Qiao, Z.Z. Sun and Z.R. Zhang, Stability and convergence of second-order schemes for the nonlinear epitaxial growth model without slope selection, *Math. Comp.*, **84** (2015), 653-674.

[34] Z.H. Qiao, T. Tang and H.H. Xie, Error analysis of a mixed finite element method for the molecular beam epitaxy model, *SIAM J. Numer. Anal.*, **53** (2015), 184-205.

[35] Z.H. Qiao, Z.R. Zhang and T. Tang, An adaptive time-stepping strategy for the molecular beam epitaxy models, *SIAM J. Sci. Comput.*, **33** (2011), 1395-1414.

[36] J. Shen, C. Wang, X.M. Wang and S.M. Wise, Second-order convex splitting schemes for gradient flows with Ehrlich-Schwoebel type energy: Application to thin film epitaxy, *SIAM J. Numer. Anal.*, **50** (2012), 105-125.

[37] J. Shen and X.F. Yang, Numerical approximations of Allen-Cahn and Cahn-Hilliard equations, *Disc. Contin. Dyn. Sys.*, **28** (2010), 1669-1691.

[38] T. Tang and J. Yang, Implicit-explicit scheme for the Allen-Cahn equation preserves the maximum principle, *J. Comput. Math.*, **34** (2016), 451-461.

[39] H.A. van der Vorst, Bi-CGSTAB: A fast and smoothly converging variant of Bi-CG for the solution of nonsymmetric linear systems, *SIAM J. Sci. Stat. Comput.*, **13** (1992), 631-644.

[40] J.B. Walsh, An introduction to stochastic partial differential equations, *Lecture Notes in Mathematics*, **1180** (1986), 265-439, Springer-Verlag. Berlin.

[41] C. Wang, X.M. Wang and S.M. Wise, Unconditionally stable schemes for equations of thin film epitaxy, *Disc. Contin. Dyn. Sys. Ser. A*, **28** (2010), 405-423.

[42] S.M. Wise, Unconditionally stable finite difference, nonlinear multigrid simulation of the Cahn-Hilliard-Hele-Shaw system of equations, *J. Sci. Comput.*, **44** (2010), 38-68.

[43] S.M. Wise, C. Wang and J.S. Lowengrub, An energy-stable and convergent finite-difference scheme for the phase field crystal equation, *SIAM J. Numer. Anal.*, **47** (2009), 2269-2288.

[44] P. van de Witte, P.J. Dijkstra, J.W.A. van den Berg and J. Feijen, Phase separation processes in polymer solutions in relation to membrane formation, *J. Membrane Sci.*, **117** (1996), 1-31.

[45] D. Zhai and H. Zhang, Investigation on the application of the TDGL equation in macromolecular microsphere composite hydrogel, *Soft Matter*, **9** (2013), 820-825.

[46] S. Zhang and M. Wang, A nonconforming finite element method for the Cahn-Hilliard equation, *J. Comput. Phys.*, **229** (2010), 7361-7372.

[47] W. Zhang, T.J. Li and P.W. Zhang, Numerical study for the nucleation of one-dimensional stochastic Cahn-Hilliard dynamics, *Commun. Math. Sci.*, **10** (2012), 1105-1132.

[48] Z.R. Zhang and Z.H. Qiao, An adaptive time-stepping strategy for the Cahn-Hilliard equation, *Commun. Comput. Phys.*, **11** (2012), 1261-1278.